PLOS GENETICS

RESEARCH ARTICLE

A ZIP1 separation-of-function allele reveals that centromere pairing drives meiotic segregation of achiasmate chromosomes in budding yeast

Emily L. Kurdzo[1,2], Hoa H. Chuong[1], Jared M. Evatt[1,2], Dean S. Dawson[1,2]*

1 Program in Cell Cycle and Cancer Biology, Oklahoma Medical Research Foundation, Oklahoma City, OK, United States of America, **2** Department of Cell Biology, University of Oklahoma Health Sciences Center, Oklahoma City, OK, United States of America

* dawsond@omrf.org

Citation: Kurdzo EL, Chuong HH, Evatt JM, Dawson DS (2018) A ZIP1 separation-of-function allele reveals that centromere pairing drives meiotic segregation of achiasmate chromosomes in budding yeast. PLoS Genet 14(8): e1007513. https://doi.org/10.1371/journal.pgen.1007513

Editor: Beth A. Sullivan, Duke University, UNITED STATES

Received: December 22, 2017

Accepted: June 25, 2018

Published: August 9, 2018

Data Availability Statement: All relevant data are within the paper and its Supporting Information files.

Funding: The work was supported by NIGMS grant R01GM087377 to DSD. The funders had no role in study design, data collection and analysis, decision to publish, or preparation of the manuscript.

Competing interests: The authors have declared that no competing interests exist.

Abstract

In meiosis I, homologous chromosomes segregate away from each other–the first of two rounds of chromosome segregation that allow the formation of haploid gametes. In prophase I, homologous partners become joined along their length by the synaptonemal complex (SC) and crossovers form between the homologs to generate links called chiasmata. The chiasmata allow the homologs to act as a single unit, called a bivalent, as the chromosomes attach to the microtubules that will ultimately pull them away from each other at anaphase I. Recent studies, in several organisms, have shown that when the SC disassembles at the end of prophase, residual SC proteins remain at the homologous centromeres providing an additional link between the homologs. In budding yeast, this centromere pairing is correlated with improved segregation of the paired partners in anaphase. However, the causal relationship of prophase centromere pairing and subsequent disjunction in anaphase has been difficult to demonstrate as has been the relationship between SC assembly and the assembly of the centromere pairing apparatus. Here, a series of in-frame deletion mutants of the SC component Zip1 were used to address these questions. The identification of a separation-of-function allele that disrupts centromere pairing, but not SC assembly, has made it possible to demonstrate that centromere pairing and SC assembly have mechanistically distinct features and that the centromere pairing function of Zip1 drives disjunction of the paired partners in anaphase I.

Author summary

The generation of gametes requires the completion of a specialized cell division called meiosis. This division is unique in that it produces cells (gametes) with half the normal number of chromosomes (such that when two gametes fuse the normal chromosome number is restored). Chromosome number is reduced in meiosis by following a single round of chromosome duplication with two rounds of segregation. In the first round,

meiosis I, homologous chromosomes first pair with each other, then attach to cellular cables, called microtubules, that pull them to opposite sides of the cell. It has long been known that the homologous partners become linked to each other by genetic recombination in a way that helps them behave as a single unit when they attach to the microtubules that will ultimately pull them apart. Recently, it was shown, in budding yeast and other organisms, that homologous partners can also pair at their centromeres. Here we show that this centromere pairing also contributes to proper segregation of the partners away from each other at meiosis I, and demonstrate that one protein involved in this process is able to participate in multiple mechanisms that help homologous chromosomes to pair with each other before being segregated in meiosis I.

Introduction

In meiosis I, homologous chromosomes segregate away from each other–the first of two rounds of segregation that allow the formation of haploid gametes. In order to segregate from one another the homologs must first become tethered together as a unit, called a bivalent. As a single bivalent, the partners can attach to microtubules such that the centromeres of the homologs will be pulled towards opposite poles of the spindle at the first meiotic division. Crossovers between the aligned homologs provide critical links, called chiasmata, which allow the homologs to form a stable bivalent (reviewed in [1]). Failures in crossing-over are associated with elevated levels of meiotic segregation errors in many organisms, including humans (reviewed in [2]). However, there are mechanisms, other than crossing-over, that can also tether partner chromosomes. Notably, studies in yeast and mouse spermatocytes have revealed that the centromeres of partner chromosomes pair in prophase of meiosis I [3–6]. In budding yeast, it has been shown that this centromere pairing is correlated with the proper segregation of chromosome pairs that have failed to form chiasmata. But the formal demonstration that centromere pairing in prophase directly drives disjunction in anaphase has been difficult, because the mutations that disrupt centromere pairing also disrupt other critical meiotic processes [7, 8].

The protein Zip1 in budding yeast localizes to paired centromeres in meiotic prophase and is necessary for centromere pairing (Fig 1A) [7–10], and similar observations have been made in Drosophila oocytes and mouse spermatocytes [3, 6, 11]. Zip1 is expressed early in meiosis and first appears as dispersed punctate foci in the nucleus. Some, but not all, of these foci co-localize with centromeres, and indeed, Zip1 mediates the homology-independent association of centromeres at this stage of meiosis, a phenomenon called centromere-coupling (Fig 1A, green arrowhead) [10, 12]. Zip1 later acts as a component of the synaptonemal complex (SC)–a proteinaceous structure that assembles between the axes of the homologous partners as they become aligned in meiotic prophase (Fig 1A, blue arrowhead) [13]. In budding yeast and mouse spermatocytes, when the SC disassembles in late prophase Zip1/SYCP1 remains at the paired centromeres, leaving the homologous partners visibly joined by only chiasmata and centromere-pairing (Fig 1A) [3, 6–8]. Virtually all of the Zip1/SYCP1 appears to have left the chromosomes by the time they begin attaching to the meiotic spindles. The prophase association promoted by Zip1 is correlated with proper segregation in anaphase, as *zip1* deletion mutants have no centromere pairing and also segregate achiasmate partners randomly (Fig 1A) [7, 8].

A critical study by Tung & Roeder identified functional domains of Zip1 that are required for SC assembly contributing key information that has contributed to the current model for

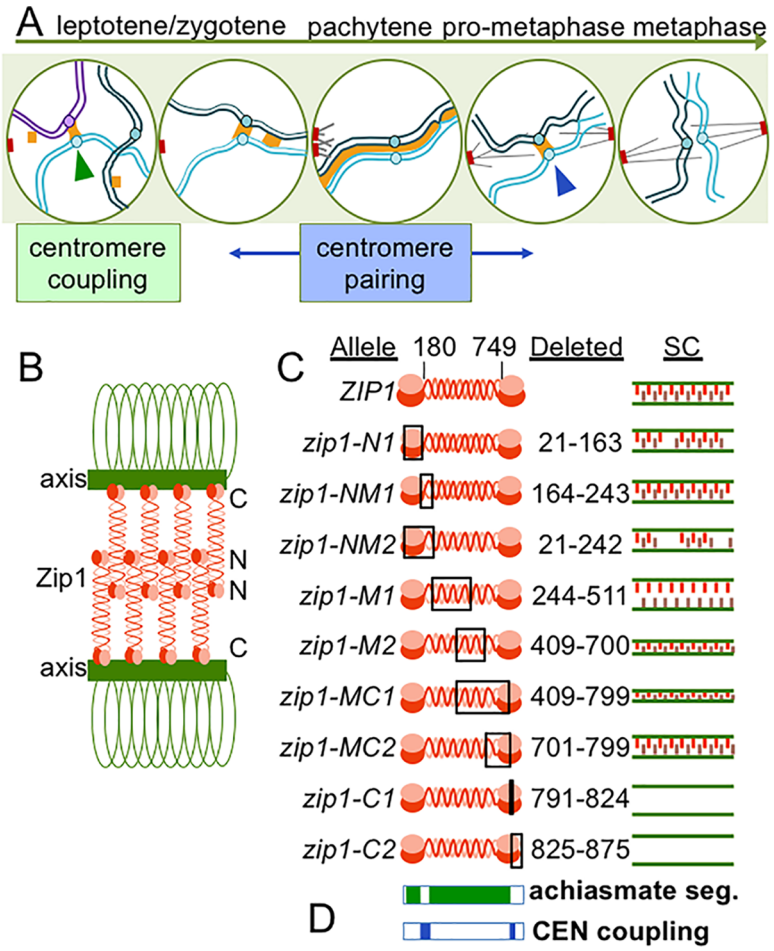

Fig 1. Meiotic centromere behaviors in budding yeast. A. In meiosis of budding yeast, Zip1 (orange) mediates centromere coupling (green arrowheads) between non-homologous partner chromosomes (light blue and purple). As the cell proceeds through later stages of meiosis, homologs pair and the mature synaptonemal complex (SC) structure zips the chromosomes together. After pachytene, the SC disassembles, except at the centromeres (blue arrowhead). **B.** The Zip1 protein is predicted to have globular domains at its ends spanning a longer coiled-coil and forms parallel dimers with N-termini in the center of the SC (denoted by N) and the C-termini along the axial elements (denoted by C). **C.** We evaluated the same nine *ZIP1* deletion mutants previously described by Tung and colleagues (Tung & Roeder, 1998). The mutations are named for their relative position along the genetic sequence–N for N-terminus, M for middle region, and C for C-terminus. The approximate SC structure formed in each mutant as described by Tung and Roeder (1998) is shown. **D.** The areas shaded in blue correspond to deletions (above) that significantly disrupted centromere coupling. Those shaded in green correlate with deletions that significantly disrupted achiasmate segregation. Note that not all deletions were screened for achiasmate segregation defects because some caused a meiotic arrest.

https://doi.org/10.1371/journal.pgen.1007513.g001

the structure of the SC [14]. This and other studies [15] have suggested that in the SC, Zip1 is in the form of head-to-head dimers (Fig 1B). These dimers, in turn are thought to assemble in a ladder-like structure with the N-termini in the center of the SC and the C-termini associated with the axes of the homologous partners (Fig 1B). This model has been extrapolated to other organisms because the basic structure of transverse filament components, like Zip1, are believed to be conserved even though their amino acid sequences have diverged (reviewed in [16]).

Tung and Roeder (1998) used an ordered series of in-frame deletions of *ZIP1* to identify ways in which different regions of the protein contributed to SC structure and function (Fig

1C). This was before the discovery that Zip1 is also involved in promoting centromere coupling and centromere pairing. We have re-constructed this deletion series to evaluate the ways in which different regions of Zip1 contribute to these centromere-associated functions. This information could be used to reveal relationships in the underlying mechanisms of centromere coupling, centromere pairing, and SC assembly, and identify separation-of-function alleles that would reveal more contributions made to these processes by specific sub-regions of Zip1. These approaches make clear that centromere coupling, centromere pairing, and SC assembly all require certain parts of the Zip1 protein that are not required by the others–suggesting mechanistic differences in these phenomena (Fig 1D). Second, they provide a clear demonstration that centromere pairing in prophase, distinct from other SC-related functions of Zip1, drives disjunction of achiasmate partner chromosomes in anaphase I.

Results

The N and C terminal globular domains of Zip1 are essential for centromere coupling

A series of nine in-frame deletion mutants (Fig 1C) were tested to determine which regions of the *ZIP1* coding sequence are essential for the homology independent centromere coupling that occurs in early meiotic prophase. Centromere coupling was assayed by monitoring the numbers of kinetochore foci (Mtw1-MYC) in chromosome spreads from prophase meiotic cells [10, 12] (Fig 2A). Diploid yeast have sixteen pairs of homologous chromosomes. When the centromeres of the thirty-two chromosomes are coupled they form on average sixteen Mtw1-MYC foci (Fig 2B, *ZIP1*, blue line). Mutants that are defective in coupling exhibit higher numbers of Mtw1-MYC foci. In this and previous studies [17] we see that deletion of *ZIP1* results in average of about nineteen-to-twenty foci per strain (Fig 2B, *zip1Δ*, red line) less than the maximum of thirty-two expected if centromere coupling was abolished. This may reflect overlap of some of the centromeres, associations of centromeres by a Zip1-independent mechanism, or failure to score some of the unpaired centromeres, as the fluorescence signal is reduced by half for unpaired centromeres. However, in our hands and elsewhere [9, 10, 12, 17–19], the *zip1* deletion strain consistently yields significantly higher numbers of centromere foci in chromosome spreads, thus providing a reliable assay for centromere coupling. The experiment was done in strains lacking *SPO11*, which encodes the endonuclease responsible for creating programmed double strand DNA [20]). This blocks meiotic progression beyond the coupling stage and prevents the homologous alignment of chromosomes [12, 18]. The strains also featured GFP-tagged copies of the centromeres of chromosome I. Briefly, 256 repeats of the *lac* operon sequence (lacO) were inserted adjacent to the centromere of chromosome I (*CEN1*) and the cells were engineered to express lacI-GFP, which localizes to the lacO array [21]. In the centromere coupling stage, the two CEN1-GFP foci are nearly always separate because coupling is usually between non-homologous partner chromosomes (Fig 2A) [10].

The mutants could be assigned to one of three groups based on their coupling phenotypes (Fig 2B and S2 Table), indistinguishable from *ZIP1* (proficient for coupling; blue histograms), indistinguishable from *zip1Δ* (loss of coupling; red and orange histograms), or intermediate (green histogram) (Fig 2B). The results make it possible to assign functional roles to several portions of Zip1. First, a portion of the N-terminus and adjacent coiled-coil (NM1 region, amino acids 164–242) is critical for centromere coupling (Fig 1D). This region was shown previously to be largely dispensable for SC assembly and sporulation [14]. Second, a portion of the C-terminus (C1 region, amino acids 791–824) shown previously to be essential for SC assembly [14], is also critical for centromere coupling. Third, two mutants that are unable to

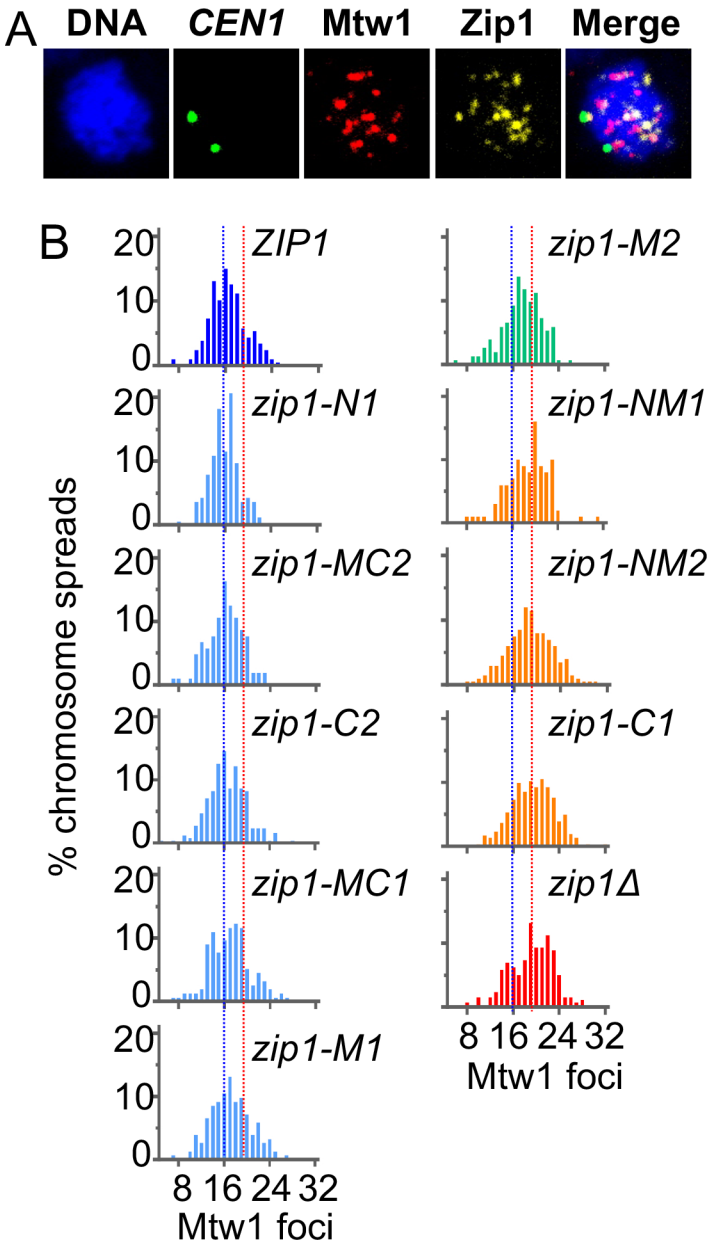

Fig 2. Centromere coupling requires parts of the N and C-termini of Zip1. A. Centromere coupling values were obtained by scoring the number of Mtw1-GFP foci in meiotic chromosome spreads. *CEN1* loci were visualized by virtue of lacI-GFP localized to a *lac* operator array next to the centromere. **B.** Coupling data. Mutants are listed according to the severity of their coupling phenotype. The thin blue and red lines indicate average Mtw1 foci values for wild-type and *zip1Δ*, respectively. The mutants were split into three groups–like wild-type (light blue), intermediate (green), and like *zip1Δ* (orange). The "like wild-type" group had values indistinguishable from wild-type but were significantly different from *zip1Δ* ($p<0.05$); whereas the "like *zip1Δ*" group had values indistinguishable from *zip1Δ* but significantly different from wild-type ($p<0.05$). The *zip1-M2* mutant had an intermediate phenotype that was significantly different from both wild-type and *zip1Δ*. A complete list of averages and statistical values are presented in S2 Table.

https://doi.org/10.1371/journal.pgen.1007513.g002

assemble SC (*zip1-C2* and *zip1-M1*; [14]) are indistinguishable from wild-type cells for centromere coupling. We conclude that Zip1 contains some regions that are critical for centromere coupling but not SC formation and vice versa.

The N-terminus of Zip1 is essential for promoting the segregation of achiasmate partners

Though centromere coupling and centromere pairing both require Zip1, they have distinct genetic requirements suggesting they may operate by (at least partially) different mechanisms [17]. To determine the regions of Zip1 that are required for achiasmate segregation we monitored the meiotic segregation of a pair of centromere plasmids that act as achiasmate partners in meiosis. Each plasmid carries an origin of DNA replication and the centromere of chromosome *III*, allowing the plasmids to behave as single copy mini-chromosomes in yeast. One plasmid is tagged with tdTomato-tetR hybrid proteins at a *tet* operon operator array [22], the other is tagged with GFP, as described above for chromosome I. Previous work has shown that such achiasmate model chromosomes disjoin properly in most meioses [23–25] and this segregation at anaphase I is correlated with the ability of their centromeres to pair late in prophase [5]. To increase the synchrony of meiotic progression in this experiment, *NDT80*, which promotes the transition out of prophase and into pro-metaphase, was placed under the control of an estradiol-inducible promotor [26–28]. Meiotic cells were allowed to accumulate in pachytene of prophase, then induced to synchronously exit pachytene and enter pro-metaphase. We scored segregation of the plasmids in the first meiotic division by monitoring the location of their GFP and tdTomato-tagged centromeres in anaphase I cells, identified by their two separated chromatin masses (Fig 3A).

Wild-type cells, under these conditions, exhibited 28% non-disjunction of the CEN plasmid pair (Fig 3B). The loss of Zip1 function can result in a pachytene arrest in some strain backgrounds [29] including the strain used in these experiments. Reducing the sporulation temperature to 23˚C, as was done here, can permit a partial bypass of the arrest [29]. Still several of the mutations (*zip1Δ*, *zip1-C2*, *zip1-C1*, and *zip1-NM2*) yielded very few anaphase cells, and failed to sporulate, presumably due to the pachytene arrest. These observations are consistent with previously published work [14]. Of the remaining mutants, three (*zip1-N1*, *zip1-M1*, *zip1-MC1)* showed significantly elevated non-disjunction of the centromere plasmids (Fig 3B) (Fig 1D). Among these three the *zip1-N1* was of particular interest. The *zip1-M1* and *zip1-MC1* mutants have disruptions in multiple processes related to Zip1 function including SC assembly, meiotic crossing-over and meiotic progression [14], thus with these mutants it would be difficult to resolve whether the observed increase in achaismate segregation is due to a specific failure in centromere behavior or a more general deficit in Zip1 activity. In contrast, the *zip1-N1* mutants appear to be proficient for the essential meiotic functions of Zip1. Previous work had shown that *zip1-N1* mutants exhibit sporulation efficiency, meiotic recombination behavior, and spore viability distinguishable from WT strains [14]. This work also suggested that in *zip1-N1* mutants Zip1 deposition in SC is less continuous than in wild-type cells. Super-resolution microscopy revealed this to be true in our strain background as well (S1 Fig) and quantification of Zip1 deposition revealed that in *zip1-N1* mutants SC is characterized by more, and shorter, patches of Zip1 (S2 Fig). This reduction in Zip1 loading is not due to a dramatic reduction of Zip1 expression or stability in the *zip1-N1* strains (S3 Fig). As in previous studies spore viability in *zip1-N1* mutants was indistinguishable from wild-type strains suggesting that chromosome segregation occurs with high fidelity in *zip1-N1* mutants (S2 Fig). Together the *zip1-N1* phenotypes suggest that amino acids 21–163 (deleted in *zip1-N*1) are more critical for mediating the segregation of achiasmate partners than for other aspects of SC assembly and function. For this reason, we focused our further analyses on this allele.

Because achiasmate segregation in anaphase is correlated with prior centromere pairing in prophase [7, 8], we tested whether the *zip1-N1* mutants were proficient in centromere pairing. Wild-type and *zip1-N1* cells containing GFP and tdTomato tagged centromere plasmids were

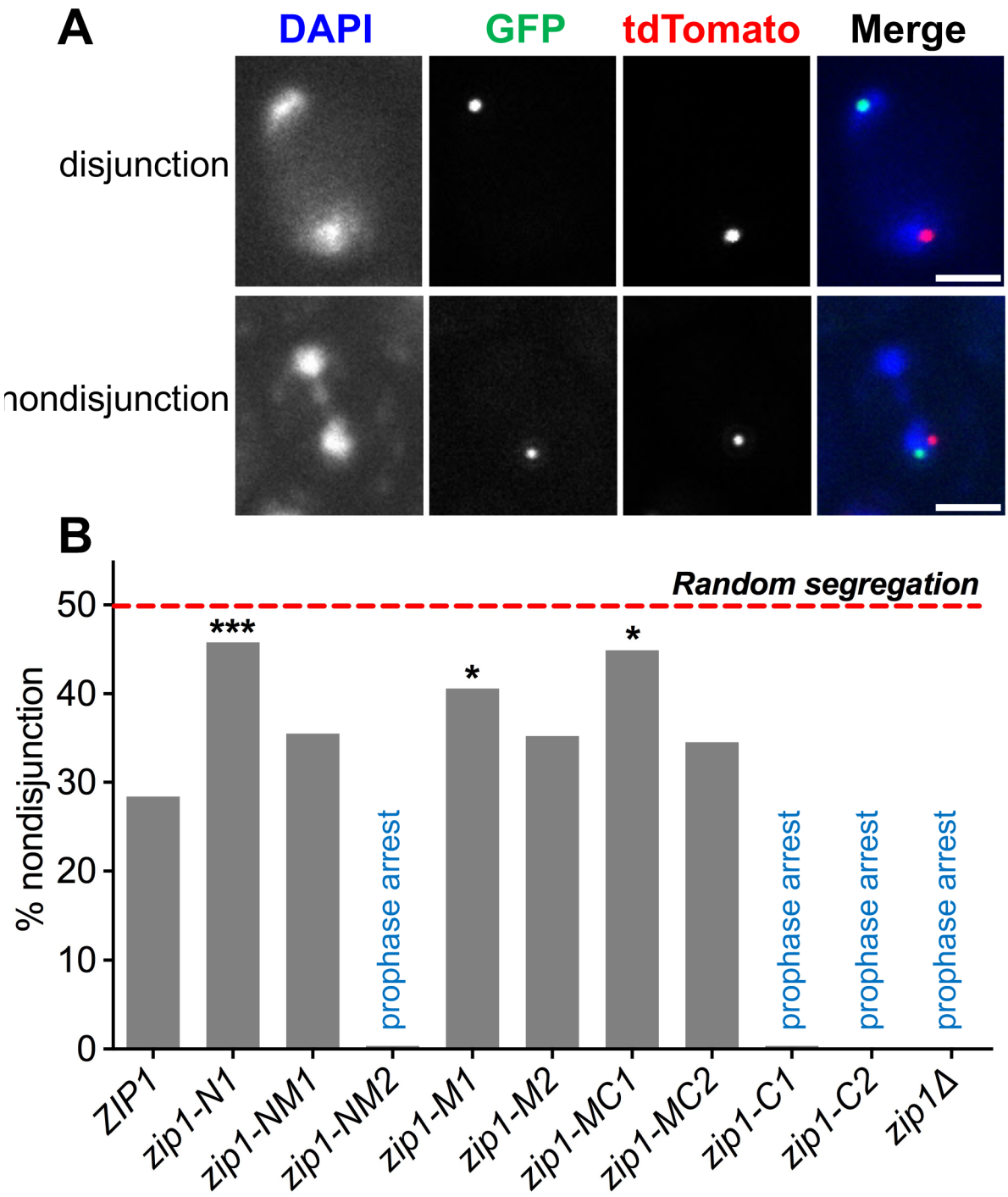

Fig 3. Centromere plasmid disjunction requires the N-terminus of Zip1. A. Representative binucleate cells with disjoined (a *ZIP1* cell) and non-disjoined (a *zip1-N1* cell) centromere plasmids. The segregation of CEN plasmids in anaphase I was assessed by monitoring the tetR-tdTomato and lacI-GFP foci localized to *tet* and *lac* operator repeats, respectively, inserted into a plasmid that contains 5.1 kb of *CEN3* sequence. **B.** Non-disjunction frequencies for CEN plasmids in each strain. n values: *ZIP1*, 250; *zip1-N1*, 190; *zip1- NM1*, 200; *zip1-M1*, 143; *zip1-M2*, 54; *zip1-MC1*, 69; *zip1-MC2*, 55. Statistical comparisons were performed with Fisher's exact test to compare all genotypes to WT. Bonferroni's correction was utilized to adjust for the number of comparisons. $^{*}p \leq 0.05$.; $^{***}p \leq 0.00625$. Scale bars equal 2 μm.

https://doi.org/10.1371/journal.pgen.1007513.g003

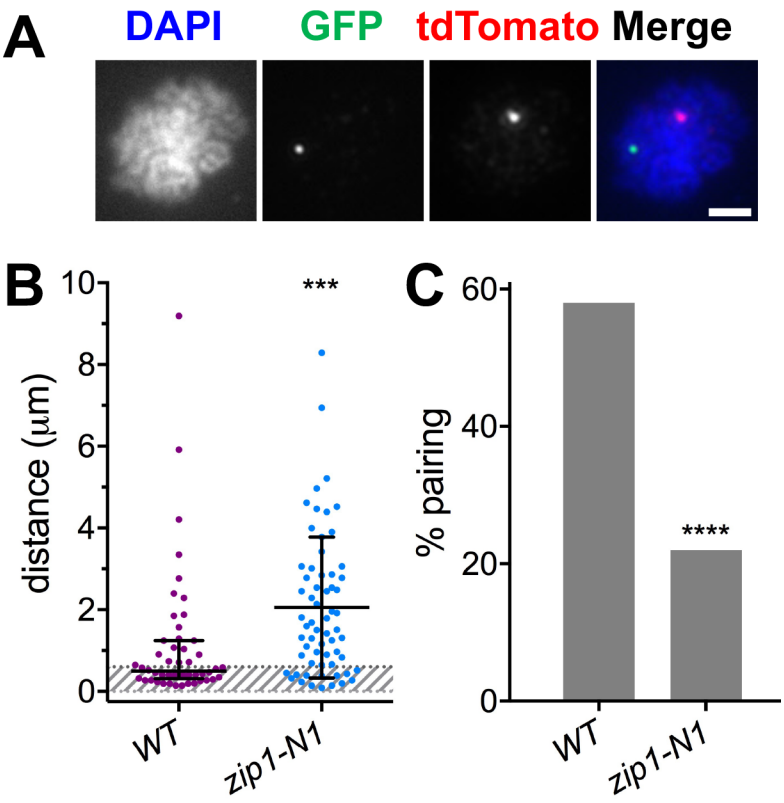

Fig 4. Centromere plasmid pairing requires the N-terminus of Zip1. Pairing of plasmid centromeres in prophase chromosome spreads was assessed by monitoring the pairing of tetR-tdTomato and lacI-GFP foci localized to *tet* operator and *lac* operator arrays on plasmids bearing a 5.1 kb region of chromosome *III* encompassing *CEN3*. **A.** An example of a spread with unpaired plasmid centromeres. **B.** Distances between the centers of the tdTomato and GFP foci in each spread (average and standard deviation). *** P = 0.0002. The grey cross-hatched region indicates separation of less-than 0.6 μm between the centers of the foci, a distance used to infer pairing of the centromeres. **C.** The percent of spreads scored as "paired" in the *ZIP1* (58%, n = 50) and *zip1-N1* (22%, n = 63) strains. ****p<0.0001. Scale bar equals 2 μm.

https://doi.org/10.1371/journal.pgen.1007513.g004

induced to sporulate and harvested five—seven hours later when pachytene cells are prevalent. Chromosome spreads were then prepared and the distances between the tdTomato and GFP foci were measured in spreads exhibiting the condensed chromatin typical of pachytene cells (Fig 4A). The average centromere-centromere distance was significantly greater in *zip1-N1* mutants (Fig 4B) consistent with a loss of pairing. When spreads with an inter-centromere distance of less than 0.6 μm were scored as "paired" (see example in Fig 4A), the *zip1-N1* mutation was found to exhibit a significant reduction in the frequency centromere pairing between the achiasmate plasmids (Fig 4C).

The N-terminus of Zip1 is necessary for efficient localization to kinetochores

Failure of centromere pairing in the *zip1-N1* mutant could be due to a failure of Zip1 to associate with centromeres. To test this, we analyzed the co-localization of the Zip protein with kinetochores in *ZIP1* and *zip1-N1* strains. The experiments were done in a *zip4Δ* strain background to allow visualization of Zip1 localization independently of an SC structure. Images were collected using structured illumination microscopy and the level of co-localization was determined (see Materials and Methods). Briefly, the images of Mtw1 and Zip1 were converted

to binay images and the overlap of the Mtw1 and Zip1 foci was determined using ImageJ software and the plug-in JACoP [30]. The positions of the foci were then computationally randomized within the area of the chromosome spread one thousand times, and Costes' P-value was then calculated to evaluate the statistical significance of the difference between the frequency of observed versus random overlap [31]. Every *ZIP1* spread showed significantly more co-localization of Zip1 and Mtw1 than was found in a randomized simulation (Fig 5A), consistent with earlier work [9, 10, 12]. By contrast, many of the *zip1-N1* spreads showed no significant co-localization above the randomized control (Fig 5B). Consistent with these results, *zip1-N1* chromosome spreads, as a group, showed significantly lower levels of co-localization of Mtw1 with Zip1 than was seen in *ZIP1* strains (Fig 5C).

The N-terminus of Zip1 is necessary for the pairing of natural chromosomes

The reduced localization of Zip1-N1 protein to natural centromeres, above, and the failure of pairing of plasmid centromeres in *zip1-N1* strains (Fig 4) raised the question of whether the *zip1-N1* mutation compromises the pairing of natural chromosomes. To assay centromere pairing we counted the numbers of kinetochore foci (Mtw1-GFP) in chromosome spreads from *ZIP1*, *zip1-N1* and *zip1Δ* cells, in the above experiment (Fig 5) using structured illumination microscopy. Prior work had shown that in *zip4* mutants, with no SC, kinetochores are held in close proximity by centromere pairing. When *ZIP1* is deleted, the centromeres can resolve into two foci in chromosome spreads [32]. The *ZIP1* strain gave an average of 13.9 kinetochore foci per spread, consistent with pairing of the 32 kinetochores. The *zip1-N1* mutant gave significantly higher numbers of kinetochore foci (average 16.4; $p<0.01$) signifying a loss of centromere pairing but not as dramatic a loss was observed in the *zip1* strain (average 21.3; $p<0.0001$).

Discussion

Our analysis of a set of in-frame Zip1 deletions has added to our understanding of the functional domains of the Zip1 protein, helping to ascribe particular Zip1 functions to specific regions of the protein. Zip1 is critical for SC assembly and processes that depend on SC assembly, including crossover formation and progression through pachytene [29]. More recently it has become clear that Zip1 acts at centromeres both early in prophase, where centromeres become associated in a homology-independent fashion (centromere coupling), and later when homologous centromeres, or the centromeres of achiasmate chromosomes, become associated by remnants of the SC that remain at the centromeres after SC disassembly (reviewed in [33]). The experiments here were intended to clarify whether SC assembly, centromere coupling, and centromere pairing incorporate Zip1 in the same or different mechanisms, and if there are differences in the regions of Zip1 that are critical to each function.

Centromere coupling and SC assembly

Prior work has shown convincingly that the structure that mediates centromere coupling is distinct from mature SC [9, 10, 17, 19]. Several proteins (Zip2, Zip3, Zip4, Ecm11, Gmc2, and Red1) known to be essential for SC assembly are not required for centromere coupling. But the domains of Zip1 that are required for centromere coupling have not been defined. The experiments here reinforce that the requirements for Zip1 for centromere coupling and SC assembly are quite different. First, centromere coupling was proficient in *zip1-C2* mutants, which have severe defects in SC assembly. But these mutants exhibit little Zip1 expression, which may be due to the lack of a nuclear localization signal [34]. Thus, this result is difficult

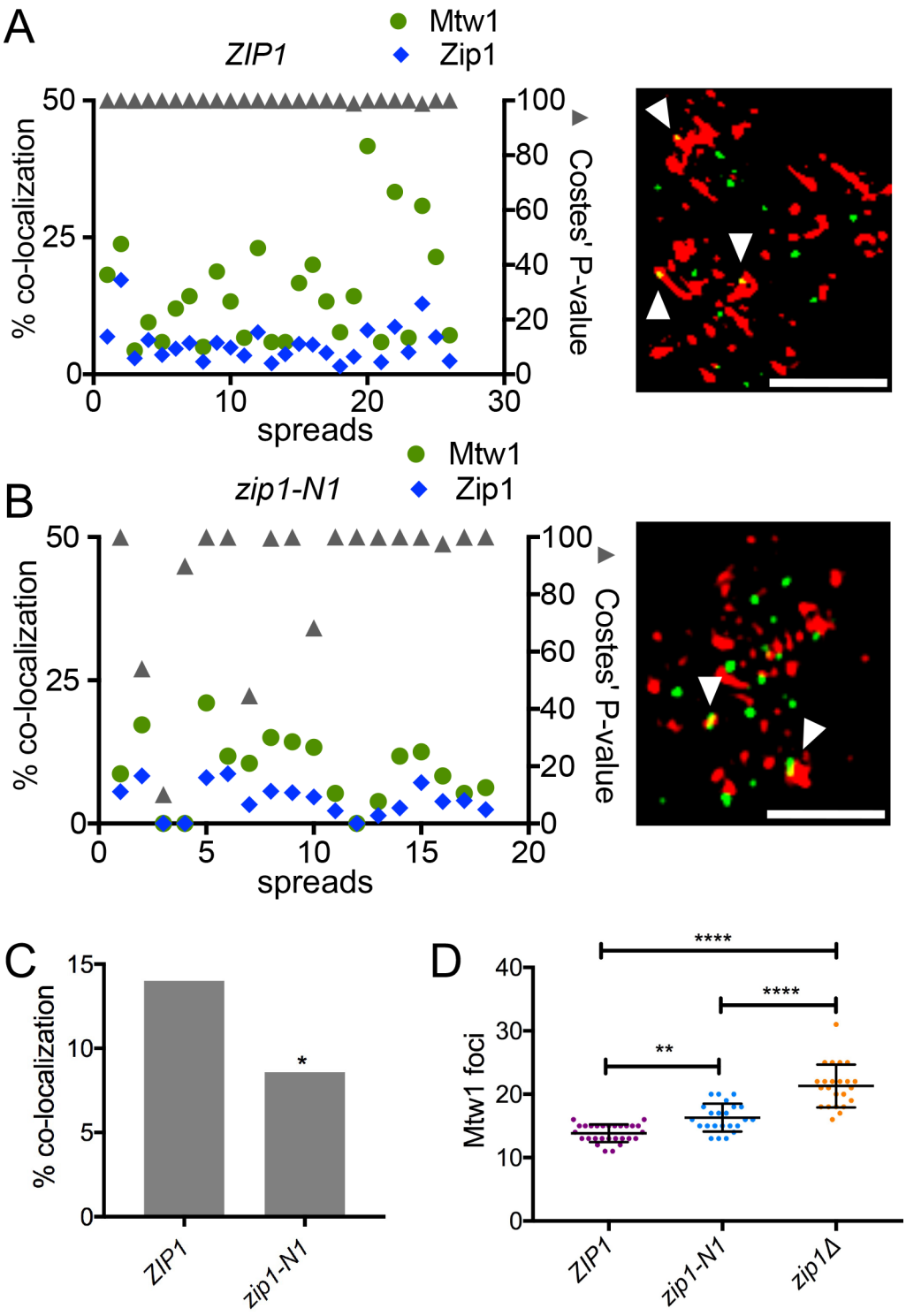

Fig 5. The Zip1 N-terminal domain is required for efficient co-localization to centromeres. Chromosome spreads were prepared from prophase *ZIP1* and *zip1-N1* cells expressing Mtw1-GFP as a kinetochore marker. Indirect fluorescence structured illumination microscopy was used to visualize Mtw1-GFP and Zip1 foci (Zip1 antibodies were raised against carboxy-terminal amino acids shared by both the wildtype and Zip1-N1 proteins). **A and B.** The overlap of Mtw1 foci with Zip1 foci (green circles) and Zip1 foci with Mtw1 foci (blue circles) was measured in each spread and the statistical significance of the difference between the observed Mtw1 co-localization with Zip1 from random simulations was evaluated with Costes' P-value (gray triangles; greater than 95% is considered significant). Representative images from the two strains are shown. Zip1 (red), Mtw1-GFP (green), overlapping foci (white

arrowhead), scale bars equal 2 μm. **C.** The average co-localization of Mtw1 foci with Zip1 across all the chromosome spreads was determined. * $p<0.05$. **D.** Centromere pairing was evaluated by counting the number of Mtw1-GFP foci in the chromosome spreads. *ZIP1* (n = 27), *zip1-N1* (n = 22), *zip1Δ* (n = 22). **$P<0.01$, ****$P<0.0001$.

https://doi.org/10.1371/journal.pgen.1007513.g005

to interpret other than to suggest that centromere coupling may require far less Zip1 than does SC assembly. Notably, the *zip1-M1* mutation, which also blocks SC assembly, is proficient in centromere coupling. The *zip1-M1* mutation, which eliminates amino acids 244–511, has a unique SC defect. The Zip1-M1 protein efficiently localizes to the axes of the homologous partners, but does not efficiently cross-bridge the axes (Fig 1C; [14]). This defect may reflect an inability of Zip1 molecules from opposite axes to associate with one another (as in Fig 1B) or may reflect an inability of Zip1 to associate with central element proteins that promote or stabilize the cross-bridging of axes by Zip1. In either case, such cross-bridging must not be important for centromere coupling, and is consistent with the finding that the central element proteins Ecm11 and Gmc2 are also not required for centromere coupling [19]. Together these findings suggest that centromere coupling is probably not mediated by a structure that includes SC-like cross-bridging. The only protein, beyond Zip1, that is known to be required for centromere coupling is the cohesin component Rec8 [9] (the requirements for the other cohesin subunits have yet to be reported). It may be that centromere coupling is mediated by the cohesin-dependent accumulation of Zip1 at early prophase centromeres [9, 32], followed by interactions between Zip1 molecules that promote the association of centromere pairs.

Centromere pairing and SC assembly

Experiments performed mainly in a mouse spermatocyte model [3, 6] suggest that the SYCP1 (the functional homolog of Zip1) that persists at paired centromeres, after SC disassembly, is accompanied by other SC proteins. This suggests that centromere pairing could be mediated by a conventional SC structure. But the identity of regions of Zip1 that are critical for centromere pairing, and whether they are distinct from the regions necessary for SC assembly, have not been addressed. Our work suggests that there are significant differences in the requirements for Zip1 function in centromere pairing and SC assembly. We arrive at this conclusion following an evaluation of the centromere pairing phenotypes of the *zip1-N1* in-frame deletion. Prior work had shown this allele had no measurable differences from the wild-type *ZIP1* allele in spore viability, crossover frequency, and genetic interference, with a slight defect in the continuity of mature linear SC structures [14]. In our strain background the *zip1-N1* mutation also exhibited wild-type levels of spore viability, and structured illumination microscopy confirmed the slight discontinuity in some SC structures in the *zip1-N1* background (S1 Fig and S2 Fig.). However, in centromere pairing assays the *zip1-N1* mutants showed major defects. In the *zip1-N1* mutant the centromeres of natural chromosome bivalents were more likely to become disengaged in chromosome spreads than was seen with wild-type controls, but the defect was not as severe as is seen in *zip1Δ* strains–suggesting that there are regions outside of the N1 region that also promote association of the bivalent centromeres. It could be that these other regions are influencing things like cross-over frequency or distribution, that along with centromere-pairing help keep bivalent centromeres associated in the natural chromosome pairing assays. When we assayed the segregation of achiasmate centromere plasmids, in which such functions cannot contribute to centromere association, then the *zip1-N1* phenotype becomes severe. The *zip1-N1* mutant showed a dramatic reduction in the pairing of plasmid centromeres. In the systematic analysis of SC assembly in the *ZIP1* deletion mutants performed by the Roeder laboratory [14], *zip1-N1* mutants assembled SC with apparently normal kinetics. Our imaging analysis reveals that in *zip1-N1* mutants, some chromosomes exhibit

SC that features discontinuous deposition of. Zip1 while others exhibit SC that is undistinguishable from that on wild-type chromosomes. Further this SC is sufficient to promote high fidelity segregation of exchange chromosomes. In contrast, the Zip1-N1 protein is completely defective for achiasmate centromere pairing, suggesting that the centromere pairing defect isn't just due to inefficient SC assembly. Instead, the sensitivity of centromere pairing to the *zip1-N1* mutation suggests that the N-terminus imbues functions on the protein that are especially or specifically important for centromere pairing. The mechanism of centromere pairing remains unclear as does the role of the Zip1 N-terminus, but kinetochore co-localization experiments suggest that this region of Zip1 promotes localization to, or maintenance of, Zip1 at the centromeres in late prophase. The fact that early prophase centromere coupling is normal in *zip1-N1* mutants reinforces that coupling and pairing are fundamentally distinct processes and that the N1 region is not necessary for localization of Zip1 to centromeres in early prophase when coupling occurs.

Meiotic prophase centromere pairing drives achiasmate disjunction

Experiments in yeast, *Drosophila* and mice have shown that SC-related proteins persist at paired centromeres after SC disassembly [3, 7, 8, 11]. These observations have been the foundation for the model that centromere pairing promotes subsequent disjunction, especially of achiasmate chromosomes that are only connected at their centromeres. Until this work, it has not been possible to conclusively demonstrate a causal relationship between centromere pairing and non-exchange disjunction, because the genetic analysis of this relationship used mutations that disrupted multiple meiotic processes–not just centromere pairing. The *zip1-N1* separation-of-function allele, because it is indistinguishable from wild-type for most assayable functions of Zip1, has made it possible to formally demonstrate that centromere-pairing in prophase is a requisite step in a process that mediates the segregation of achiasmate partners in anaphase.

The mechanistic question of how prophase centromere pairing drives disjunction remains to be answered. The fact that in yeast, mice and *Drosophila*, the majority of the centromeric SC components have been lost from the centromeres well before the partners begin to attach to microtubules makes this even more mysterious. The *zip1-N1* allele, which specifically targets centromere associations of Zip1, and the centromere pairing process, will be an important tool for addressing these questions.

Materials and methods

Strains

We created the same nine deletion mutants of *ZIP1* that Tung and Roeder had studied for their work in SC formation [14] by using standard PCR and two-step-gene-replacement methods [35, 36]. All mutant versions of *ZIP1* were confirmed by PCR and sequencing. The native *ZIP1* promoter was unaltered in these strains allowing each mutant protein to be expressed at the appropriate level and time. Culturing of strains was as described previously [17]. Strain genotypes are listed in S1 Table.

Centromere coupling assay

Centromere coupling was monitored largely as described previously [12]. Cells were harvested five hours after shifting cultures to sporulation medium at 30˚C. Meiotic nuclear spreads were prepared according to [37] with minor modifications. Cells were spheroplasted using 20 mg/ml zymolyase 100T for approximately 30 minutes. Spheroplasts were briefly suspended in

MEM (100mM MES, 10mM EDTA, 500μM $MgCl_2$) containing 1mM PMSF (phenylmethylsulfonyl fluoride), fixed with 4% paraformaldehyde plus 0.1% Tween20 and spread onto poly-L-lysine-coated slides (Fisherbrand Superfrost Plus). Slides were blocked with 4% non-fat dry milk in phosphate buffered saline for at least 30 minutes, and incubated overnight at 4˚C with primary antibodies. Primary antibodies were mouse anti-Zip1 (used at 1:1000 dilution), rabbit anti-Zip1 (used at 1:1000 dilution; Santa Cruz y-300 SC-33733), rabbit anti-MYC (1:400; Bethyl Laboratories A190-105A), mouse anti-MYC (used at 1:1000 dilution; gift from S. Rankin), chicken anti-GFP (used at 1:500 dilution; Millipore AB16901), rabbit anti-DsRed (used at 1:1000–1:2000 dilution; Clontech 632496), and rabbit anti-RFP (1:500; Thermo Scientific 600-401-379). Secondary antibodies were obtained from Thermo Fisher: Alexa Fluor 488-conjugated goat anti-chicken IgG (used at 1:1200 dilution), Alexa Fluor 568-conjugated goat anti-mouse IgG (1:1000), Alexa Fluor 647 conjugated goat anti-rabbit IgG (used at 1:1200 dilution), and Alexa Fluor 568-conjugated goat anti-rabbit IgG (used at 1:1000 dilution).

Mtw1 (an inner kinetochore protein) foci (Mtw1-13xMYC) were quantified in spreads with an area of 15 μm^2 or more to ensure centromeres were spread enough to assay. Centromere coupling would theoretically yield 16 kinetochore (Mtw1) foci while complete absence of coupling would yield 32 kinetochore foci. All strains were *spo11Δ*/*spo11Δ* to block progression beyond the coupling stage [12, 18]. The individual performing the scoring was blinded to the identity of the mutation. The average number of Mtw1 foci seen in the chromosome spreads of each in-frame deletion strain was compared to the values obtained from the *ZIP1* and *zip1Δ* control strains, using the Kruskal-Wallis test, performed using Prism 6.0. The statistical data for the experiment are reported in S2 Table.

Achiasmate segregation assay

Non-disjunction frequencies of centromere plasmids were determined in a manner similar to previously published assays [7]. Plasmids were constructed with arrays of 256 repeats of the *lac* operator or *tet* operator sequence inserted adjacent to a 5.1 kb interval from chromosome III that includes *CEN3*. These cells expressed a *GFP-lacI* hybrid gene under the control of a meiotic promoter and a *tetR-tdTomato* hybrid gene under the control of the *URA3* promoter. This produced fluorescent foci at the operator arrays [35, 36]. Cells were sporulated at 23˚C (rather than 30˚C) as this has been shown to allow by-pass of the pachytene arrests triggered by some *ZIP1* mutations [29]. Even at this temperature cells with the *zip1-C1*, *zip1-C2*, *zip1-NM2* and *zip1Δ* mutations mainly arrested in pachytene, so no anaphase segregation data were gathered for these strains. Harvested cells were either assayed fresh or were frozen in 15% glycerol and 1% potassium acetate until the time at which they were assayed. Preparation for assaying the cells included staining the cells with DAPI and then mounting the cells on agarose pads for viewing as described previously [38]. Anaphase I cells were identified by the presence of two DAPI masses on either side of elongated cells, indicating that the chromosomes had segregated. To avoid scoring cells with duplicated or lost CEN plasmids, only cells with one GFP focus and one tdTomato focus were assayed. Images were collected using the 100X objective lens of a Zeiss AxioImager microscope with band-pass emission filters, a Roper HQ2 CCD, and AxioVision software.

Plasmid centromere pairing assay

Centromere pairing in pachytene was assessed using published methods [7] but with the centromere plasmids described above. Sporulation was done at 30˚C. Chromosome spreads were prepared as described in [39], with the following modifications: Cells were harvested 5–7 hours after induction of sporulation at 30˚C. After chromosome spreads were created and

dried overnight, the slides were rinsed gently with 0.4% Photoflo (Kodak). Each slide was then incubated with PBS/4% milk at room temperature for 30 minutes in a wet chamber. Milk was drained off of the slide, and primary antibody diluted in PBS/4% milk was incubated on the slide overnight at 4˚C. A control slide with PBS/4% milk was used for each experiment. The following day, the slides were washed in PBS, and incubated with secondary antibody diluted in PBS/4% milk for 2 hours in a wet chamber at room temperature. The slides were gently washed in PBS. DAPI (4',6-diamidino-2-phenylindole, used at 1μg/ml) was added to each slide and allowed to incubate at room temperature for 10 minutes. Slides were then washed gently in PBS and 0.4% Photoflo, then allowed to dry completely before a coverslip was mounted. Antibodies are described in the previous section. Only cells that exhibited "ropey" DAPI staining were scored in this assay, and were disqualified for assessment if there was more than one GFP focus or more than one tdTomato focus. In these cells, the distance between the center of the green focus and the center of the red focus was measured using AxioVision software. The distributions of distances in the *ZIP1* and *zip1-N1* strains were determined to be significantly different with the Kolmogorov-Smirnov test (Kolmogorov-Smirnov D = 0.4032; P = 0.0002) using the Prism 6.0 software package. As in previous work [7], foci with center-to-center distances less than or equal to 0.6 μm were scored as paired (these foci are typically touching or overlapping). The frequency of pairing (distance less than 0.6 μm) in the *ZIP1* (32 of 50) and *zip1-N1* (14 of 63) chromosome spreads was found to be significantly different ($p<0.0001$) using Fisher's Exact test performed with the Prism 6.0 software package.

Synaptonemal complex evaluation by structured illumination microscopy

Chromosome spreads were prepared according to the protocol of Grubb and colleagues [39] as described above, and harvested from sporulation cultures five hours after placing cells in sporulation medium at 30˚C. To visualize the axial elements (Red1) and transverse elements (Zip1) of the SC by indirect fluorescence microscopy, chromosome spreads were stained with following primary and secondary antibodies: guinea pig anti-Red1 antibody (1:1000), goat anti-Guinea pig Alexa 488 antibody (Invitrogen) (1:1000), and rabbit anti-Zip1 antibody (1:800), donkey anti-rabbit Alexa 568 antibody (Invitrogen) (1:1000). Chromosome spreads were imaged with a Deltavision OMX-SR structured illumination microscope (SIM).

Mtw1-Zip1 co-localization assay

Chromosome spreads were prepared according to the protocol of [39] as described above. All strains carried the *zip4Δ* to prevent SC assembly. Chromosomes were stained with primary antibodies: mouse anti-MYC (Mtw1-13xMYC) (Developmental Studies Hybridoma Bank) at 1:20 dilution and rabbit anti-Zip1 antibody at 1:1000 dilution and secondary antibodies Alexa 488 donkey anti-mouse (Invitrogen) at 1:1000 dilution and Alexa 568 goat anti-rabbit (Invitrogen) at 1:1000 dilution. Zip1 antibodies were raised against amino acids 611–875 from the carboxy terminus of Zip1, shared by both wild-type Zip1 and Zip1-N1 proteins. The Zip1-GST fusion for antibody preparation was expressed from plasmid R1640, generously provided by Shirleen Roeder [13]. Chromosome spreads were imaged with a Deltavision OMX-SR structured illumination microscope (SIM). Acquired images were converted to binary images using ImageJ software and the number of overlapping Mtw1-13xMYC and Zip1 foci were scored using the ImageJ plugin, JACoP [30]. To determine whether co-localization occurred at frequencies that were significantly higher than expected for random overlaps, given the number of Mtw1 and Zip1 foci in each image, the foci in each image were randomized in one thousand simulations using Costes' randomization in JACoP, then the frequency of random overlaps was determined and compared to the observed overlap frequency [30]. Costes' P-value was

then calculated to evaluate the statistical significance of the difference between the frequency of observed versus random overlap [31]. In addition, the average co-localization observed for all of the *ZIP1* spreads (26 spreads, 238 Mtw1 foci, 33 co-localized with Zip1) and all of the *zip1-N1* spreads (18 spreads, 279 Mtw1 foci, 12 co-localized with Zip1) was determined and the statistical significance of the difference determined using Fisher's two-tailed exact test ($p = 0.0001$). The experiment presented is one of two performed, both with the same outcome (significantly reduced Mtw1-Zip1 co-localization in the *zip1-N1* mutant).

Centromere pairing of natural chromosomes

The chromosome spreads used in the experiment above were used to assay the number of distinct Mtw1-13xMYC foci in *ZIP1*, *zip1-N1* and *zip1Δ* chromosome spreads. With complete pairing of the homologous chromosomes, the thirty-two kinetochores should appear as sixteen Mtw1-13xMYC foci. In the absence of pairing, kinetochores from the paired homologs can sometimes separate far enough to be resolved as individual foci (the homologs remain tethered by crossovers and probably other constraints), thus giving higher numbers of Mtw1-13xMYC foci–in theory up to thirty-two foci. The SIM images described in the preceding section were converted to binary images using ImageJ software and the number of Mtw1-13xMYC foci tallied for each spread using the Analyze Particles function in ImageJ. The average number of Mtw1-13xMYC foci per spread was determined for each genotype (*ZIP1*, *zip1-N1*, and *zip1Δ)* and the statistical significance of the observed differences between the genotypes was calculated with one-way ANOVA and multiplicity adjusted P values were obtained with Sidak's multiple comparisons testing using Prism 7.0.

Western blots

To induce meiosis, diploid cells were grown in YP-acetate for 18 hours and then shifted to 1% potassium acetate sporulation medium at $1x10^8$ cells/ml. Following transfer to sporulation medium, 0.5 ml of culture was harvested at 0, 3, 5, 7, 9, 11, and 24-hour time points. Cells were disrupted in cold 16.6% trichloroacetic acid and 0.5mm glass beads (Biospec Products) in a Bullet Blue Blender for 5 minutes at speed setting 8 following the manufacturer's instructions. Protein precipitates were washed in cold 95% ethanol, pelleted in a microcentrifuge, and resuspended in SDS-PAGE buffer. Samples were boiled for 10 minutes and pelleted at 16.4 x g for 15 minutes at 4˚C. Equal volumes of each sample were loaded onto 8% polyacrylamide gels in duplicate. For one gel, blotted proteins were detected using primary antibodies against Zip1 (rabbit anti-Zip1 antibody raised against the C-terminal 264 amino acids of Zip1; used at a 1:3000 dilution) and goat anti-Rabbit horse radish peroxidase (HRP) conjugated antibody (Fisher PI31460; 1:5000 dilution). For the duplicate blot, Pgk1 was detected using mouse anti-Pgk1 (Molecular Probes 22C5; used at a 1:3000 dilution) and donkey anti-Mouse HRP secondary antibody (Jackson 715-035-151, 1:5000 dilution). Images were collected on an Azure c600 Imager.

Supporting information

S1 Fig. *zip1-N1* cells assemble synaptonemal complexes and exhibit high spore viability.
(PDF)

S2 Fig. Quantifying Zip1 deposition in synaptonemal complexes of *zip1-N1* mutants.
(PDF)

S3 Fig. Western blot analysis of Zip1 and Zip1-N1 expression.
(PDF)

S1 Table. Strains used in this study.
(PDF)

S2 Table. Statistics for centromere coupling experiments.
(PDF)

Acknowledgments

We thank Marta Kasperzyk for the guinea pig Red1 antibody, Rebecca Boumil for the mouse anti-Zip1 antibody, and Jingrong Chen and Susannah Rankin for help with antibody preparation. We thank Lori Garman for help with statistical analysis. We are grateful to colleagues in the Program in Cell Cycle and Cancer Biology for helpful discussions of this work.

Author Contributions

Conceptualization: Emily L. Kurdzo, Dean S. Dawson.

Data curation: Emily L. Kurdzo, Hoa H. Chuong.

Formal analysis: Emily L. Kurdzo, Hoa H. Chuong.

Funding acquisition: Dean S. Dawson.

Investigation: Emily L. Kurdzo, Hoa H. Chuong, Jared M. Evatt.

Project administration: Dean S. Dawson.

Supervision: Dean S. Dawson.

Writing – original draft: Emily L. Kurdzo, Dean S. Dawson.

Writing – review & editing: Emily L. Kurdzo, Hoa H. Chuong, Dean S. Dawson.

References

1. Duro E, Marston AL. From equator to pole: splitting chromosomes in mitosis and meiosis. Genes Dev. 2015; 29(2):109–22. Epub 2015/01/17. https://doi.org/10.1101/gad.255554.114 PMID: 25593304; PubMed Central PMCID: PMCPMC4298131.
2. Kurdzo EL, Dawson DS. Centromere pairing—tethering partner chromosomes in meiosis I. FEBS J. 2015; 282(13):2458–70. Epub 2015/03/31. https://doi.org/10.1111/febs.13280 PMID: 25817724; PubMed Central PMCID: PMCPMC4490064.
3. Bisig CG, Guiraldelli MF, Kouznetsova A, Scherthan H, Hoog C, Dawson DS, et al. Synaptonemal complex components persist at centromeres and are required for homologous centromere pairing in mouse spermatocytes. PLoS Genet. 2012; 8(6):e1002701. Epub 2012/07/05. https://doi.org/10.1371/journal.pgen.1002701 PMID: 22761579; PubMed Central PMCID: PMCPMC3386160.
4. Ding DQ, Yamamoto A, Haraguchi T, Hiraoka Y. Dynamics of homologous chromosome pairing during meiotic prophase in fission yeast. Dev Cell. 2004; 6(3):329–41. Epub 2004/03/20. PMID: 15030757.
5. Kemp B, Boumil RM, Stewart MN, Dawson DS. A role for centromere pairing in meiotic chromosome segregation. Genes Dev. 2004; 18(16):1946–51. Epub 2004/08/04. https://doi.org/10.1101/gad.1227304 PMID: 15289462; PubMed Central PMCID: PMCPMC514173.
6. Qiao H, Chen JK, Reynolds A, Hoog C, Paddy M, Hunter N. Interplay between synaptonemal complex, homologous recombination, and centromeres during mammalian meiosis. PLoS Genet. 2012; 8(6): e1002790. Epub 2012/07/05. https://doi.org/10.1371/journal.pgen.1002790 PMID: 22761591; PubMed Central PMCID: PMCPMC3386176.
7. Gladstone MN, Obeso D, Chuong H, Dawson DS. The synaptonemal complex protein Zip1 promotes bi-orientation of centromeres at meiosis I. PLoS Genet. 2009; 5(12):e1000771. Epub 2009/12/17. https://doi.org/10.1371/journal.pgen.1000771 PMID: 20011112; PubMed Central PMCID: PMCPMC2781170.

8. Newnham L, Jordan P, Rockmill B, Roeder GS, Hoffmann E. The synaptonemal complex protein, Zip1, promotes the segregation of nonexchange chromosomes at meiosis I. Proc Natl Acad Sci U S A. 2010; 107(2):781–5. Epub 2010/01/19. https://doi.org/10.1073/pnas.0913435107 PMID: 20080752; PubMed Central PMCID: PMCPMC2818913.
9. Chuong H, Dawson DS. Meiotic cohesin promotes pairing of nonhomologous centromeres in early meiotic prophase. Mol Biol Cell. 2010; 21(11):1799–809. Epub 2010/04/09. https://doi.org/10.1091/mbc.E09-05-0392 PMID: 20375150; PubMed Central PMCID: PMCPMC2877639.
10. Tsubouchi T, Roeder GS. A synaptonemal complex protein promotes homology-independent centromere coupling. Science. 2005; 308(5723):870–3. Epub 2005/05/10. https://doi.org/10.1126/science.1108283 PMID: 15879219.
11. Takeo S, Lake CM, Morais-de-Sa E, Sunkel CE, Hawley RS. Synaptonemal complex-dependent centromeric clustering and the initiation of synapsis in Drosophila oocytes. Curr Biol. 2011; 21(21):1845–51. Epub 2011/11/01. https://doi.org/10.1016/j.cub.2011.09.044 PMID: 22036182.
12. Obeso D, Dawson DS. Temporal characterization of homology-independent centromere coupling in meiotic prophase. PLoS One. 2010; 5(4):e10336. Epub 2010/04/30. https://doi.org/10.1371/journal.pone.0010336 PMID: 20428251; PubMed Central PMCID: PMCPMC2859069.
13. Sym M, Engebrecht JA, Roeder GS. ZIP1 is a synaptonemal complex protein required for meiotic chromosome synapsis. Cell. 1993; 72(3):365–78. Epub 1993/02/12. PMID: 7916652.
14. Tung KS, Roeder GS. Meiotic chromosome morphology and behavior in zip1 mutants of Saccharomyces cerevisiae. Genetics. 1998; 149(2):817–32. Epub 1998/06/11. PMID: 9611194; PubMed Central PMCID: PMCPMC1460213.
15. Dong H, Roeder GS. Organization of the yeast Zip1 protein within the central region of the synaptonemal complex. J Cell Biol. 2000; 148(3):417–26. Epub 2000/02/09. PMID: 10662769; PubMed Central PMCID: PMCPMC2174805.
16. Watts FZ, Hoffmann E. SUMO meets meiosis: an encounter at the synaptonemal complex: SUMO chains and sumoylated proteins suggest that heterogeneous and complex interactions lie at the centre of the synaptonemal complex. Bioessays. 2011; 33(7):529–37. Epub 2011/05/19. https://doi.org/10.1002/bies.201100002 PMID: 21590786.
17. Kurdzo EL, Obeso D, Chuong H, Dawson DS. Meiotic Centromere Coupling and Pairing Function by Two Separate Mechanisms in Saccharomyces cerevisiae. Genetics. 2017; 205(2):657–71. Epub 2016/12/04. https://doi.org/10.1534/genetics.116.190264 PMID: 27913618; PubMed Central PMCID: PMCPMC5289843.
18. Falk JE, Chan AC, Hoffmann E, Hochwagen A. A Mec1- and PP4-dependent checkpoint couples centromere pairing to meiotic recombination. Dev Cell. 2010; 19(4):599–611. Epub 2010/10/19. https://doi.org/10.1016/j.devcel.2010.09.006 PMID: 20951350.
19. Humphryes N, Leung WK, Argunhan B, Terentyev Y, Dvorackova M, Tsubouchi H. The Ecm11-Gmc2 complex promotes synaptonemal complex formation through assembly of transverse filaments in budding yeast. PLoS Genet. 2013; 9(1):e1003194. Epub 2013/01/18. https://doi.org/10.1371/journal.pgen.1003194 PMID: 23326245; PubMed Central PMCID: PMCPMC3542071.
20. Keeney S, Giroux CN, Kleckner N. Meiosis-specific DNA double-strand breaks are catalyzed by Spo11, a member of a widely conserved protein family. Cell. 1997; 88(3):375–84. Epub 1997/02/07. PMID: 9039264.
21. Straight AF, Belmont AS, Robinett CC, Murray AW. GFP tagging of budding yeast chromosomes reveals that protein-protein interactions can mediate sister chromatid cohesion. Curr Biol. 1996; 6(12):1599–608. Epub 1996/12/01. PMID: 8994824.
22. Michaelis C, Ciosk R, Nasmyth K. Cohesins: chromosomal proteins that prevent premature separation of sister chromatids. Cell. 1997; 91(1):35–45. Epub 1997/10/23. PMID: 9335333.
23. Dawson DS, Murray AW, Szostak JW. An alternative pathway for meiotic chromosome segregation in yeast. Science. 1986; 234(4777):713–7. Epub 1986/11/07. PMID: 3535068.
24. Mann C, Davis RW. Meiotic disjunction of circular minichromosomes in yeast does not require DNA homology. Proc Natl Acad Sci U S A. 1986; 83(16):6017–9. Epub 1986/08/01. PMID: 3526347; PubMed Central PMCID: PMCPMC386428.
25. Sears DD, Hegemann JH, Hieter P. Meiotic recombination and segregation of human-derived artificial chromosomes in Saccharomyces cerevisiae. Proc Natl Acad Sci U S A. 1992; 89(12):5296–300. Epub 1992/06/15. PMID: 1608938; PubMed Central PMCID: PMCPMC49278.
26. Benjamin KR, Zhang C, Shokat KM, Herskowitz I. Control of landmark events in meiosis by the CDK Cdc28 and the meiosis-specific kinase Ime2. Genes Dev. 2003; 17(12):1524–39. Epub 2003/06/05. https://doi.org/10.1101/gad.1101503 PMID: 12783856; PubMed Central PMCID: PMCPMC196082.

27. Meyer RE, Kim S, Obeso D, Straight PD, Winey M, Dawson DS. Mps1 and Ipl1/Aurora B act sequentially to correctly orient chromosomes on the meiotic spindle of budding yeast. Science. 2013; 339 (6123):1071–4. https://doi.org/10.1126/science.1232518 PMID: 23371552; PubMed Central PMCID: PMCPMC3604795.

28. Carlile TM, Amon A. Meiosis I Is Established through Division-Specific Translational Control of a Cyclin. Cell. 2008; 133(2):280–91. https://doi.org/10.1016/j.cell.2008.02.032 PMID: 18423199

29. Borner GV, Kleckner N, Hunter N. Crossover/noncrossover differentiation, synaptonemal complex formation, and regulatory surveillance at the leptotene/zygotene transition of meiosis. Cell. 2004; 117 (1):29–45. Epub 2004/04/07. PMID: 15066280.

30. Bolte S, Cordelieres FP. A guided tour into subcellular colocalization analysis in light microscopy. J Microsc. 2006; 224(Pt 3):213–32. Epub 2007/01/11. https://doi.org/10.1111/j.1365-2818.2006.01706.x PMID: 17210054.

31. Costes SV, Daelemans D, Cho EH, Dobbin Z, Pavlakis G, Lockett S. Automatic and quantitative measurement of protein-protein colocalization in live cells. Biophys J. 2004; 86(6):3993–4003. Epub 2004/06/11. https://doi.org/10.1529/biophysj.103.038422 PMID: 15189895; PubMed Central PMCID: PMCPMC1304300.

32. Tsubouchi T, Macqueen AJ, Roeder GS. Initiation of meiotic chromosome synapsis at centromeres in budding yeast. Genes Dev. 2008; 22(22):3217–26. Epub 2008/12/06. https://doi.org/10.1101/gad.1709408 PMID: 19056898; PubMed Central PMCID: PMCPMC2593611.

33. Obeso D, Pezza RJ, Dawson D. Couples, pairs, and clusters: mechanisms and implications of centromere associations in meiosis. Chromosoma. 2014; 123(1–2):43–55. Epub 2013/10/16. https://doi.org/10.1007/s00412-013-0439-4 PMID: 24126501; PubMed Central PMCID: PMCPMC3969401.

34. Burns N, Grimwade B, Ross-Macdonald PB, Choi EY, Finberg K, Roeder GS, et al. Large-scale analysis of gene expression, protein localization, and gene disruption in Saccharomyces cerevisiae. Genes Dev. 1994; 8(9):1087–105. Epub 1994/05/01. PMID: 7926789.

35. Longtine MS III AM, Demarini DJ, Shah NG, Wach A, Brachat A, et al. Additional Modules for Versatile and Economical PCR-based Gene Deletion and Modification in Saccharomyces cerevisiae. Yeast. 1998; 14:953–61. https://doi.org/10.1002/(SICI)1097-0061(199807)14:10<953::AID-YEA293>3.0.CO;2-U PMID: 9717241

36. Janke C, Magiera MM, Rathfelder N, Taxis C, Reber S, Maekawa H, et al. A versatile toolbox for PCR-based tagging of yeast genes: new fluorescent proteins, more markers and promoter substitution cassettes. Yeast. 2004; 21(11):947–62. https://doi.org/10.1002/yea.1142 PMID: 15334558.

37. Dresser ME, Giroux CN. Meiotic chromosome behavior in spread preparations of yeast. J Cell Biol. 1988; 106(3):567–73. PMID: 2450094; PubMed Central PMCID: PMCPMC2115091.

38. Kim S, Meyer R, Chuong H, Dawson DS. Dual mechanisms prevent premature chromosome segregation during meiosis. Genes & development. 2013; 27(19):2139–46. https://doi.org/10.1101/gad.227454.113 PMID: 24115770; PubMed Central PMCID: PMC3850097.

39. Grubb J, Brown MS, Bishop DK. Surface Spreading and Immunostaining of Yeast Chromosomes. J Vis Exp. 2015;(102):e53081. Epub 2015/09/02. https://doi.org/10.3791/53081 PMID: 26325523; PubMed Central PMCID: PMCPMC4632477.